THE ASTROPHYSICAL JOURNAL, 293:445–458, 1985 June 15

[Ne II] OBSERVATIONS OF THE GALACTIC CENTER: EVIDENCE FOR A MASSIVE BLACK HOLE

E. SERABYN[1]
Department of Physics, University of California, Berkeley
AND
J. H. LACY[1]
Space Sciences Laboratory, University of California, Berkeley
Received 1984 October 18; accepted 1984 December 31

ABSTRACT

The velocity field within 2 pc of the galactic center has been investigated by observing the [Ne II] 12.8 μm fine-structure line emission from Sgr A West. The observations show regular variations in velocity along several of the most prominent radio continuum features, indicating that at least two of the features are large-scale flows of ionized gas. One of the flows follows a circular orbit at a galactocentric radius of ~ 1.7 pc and requires $4.7 \times 10^6\ M_\odot$ to lie within that radius. The other flow is well fitted by an eccentric orbit which approaches to within 0.5 pc the center of the Galaxy and which requires mass $\gtrsim 3.5 \times 10^6\ M_\odot$ to lie within that radius. The inferred mass distribution is too centrally concentrated to be due to an isothermal stellar cluster or to the stellar mass distribution indicated by the 2 μm flux from the region. Thus, a substantial fraction of the mass located within 1.7 pc of the center is contained in a more centrally concentrated form, most likely in a massive black hole of ~ 3–$4 \times 10^6\ M_\odot$. The best-fit orbits occur under the assumption that the center of the mass distribution is near the 2 μm source IRS 16 NE.

The circular orbit of ionized gas at $r \approx 1.7$ pc is most probably located on the inner edge of the ring of dust and neutral gas which orbits about the center of larger radii. Consequently, the source or sources of the ionization must be centrally located. Shielding of various portions of the ring from the central ionizing flux may play a role in determining the distribution of the ionized gas in Sgr A West. If so, the source of the ionization can be localized to within ~ 0.5 pc of the center. A single source of ionization with $T_{\rm eff} \approx 35{,}000$ K and $L_{\rm bol} \approx 10^7\ L_\odot$ is consistent with the ionization state of the gas in the central 3 pc, the bolometric luminosity of the central few persecs, and also the near-infrared flux from IRS 16 center. Thus, a single object may be the primary energy source for the central few parsecs of our Galaxy.

Subject headings: black holes — galaxies: Milky Way — galaxies: nuclei — infrared: sources

I. INTRODUCTION

The center of our Galaxy, although obscured at visible wavelengths, has been actively studied at infrared and radio wavelengths for a number of years (for recent reviews see Townes *et al.* 1983; Oort 1984; and Brown and Liszt 1984). Early observations of the thermal 10 μm emission from warm dust in the central 2 pc of our Galaxy (Rieke and Low 1973; and Becklin and Neugebauer 1975) showed a number of compact sources. Observations of [Ne II] 12.8 μm infrared fine-structure line emission (Lacy *et al.* 1979, 1980) indicated that the sources consist of ionized gas mixed with dust and that a unique radial velocity could be associated with each infrared source. This led to a model of the region in which a number of independent ionized gas clouds, each moving at a distinct velocity, orbit in the central gravitational field. Left undetermined was the question of whether this field is produced solely by a central stellar cluster or if a massive central object is also present.

Longer wavelength (100 μm) emission from cooler dust and neutral gas has been found to be localized along the galactic plane on either side of the central 3 pc region (Becklin, Gatley, and Werner 1982; Genzel *et al.* 1984). The double-lobed structure of the emission indicates the presence of a ring of gas and dust, with a lack of material in the central region, while the neutral oxygen velocities indicate that the ring is rotating about the center. The ionized gas clouds occupy only a small fraction of the volume of the central cavity, leaving most of the central 3 pc relatively transparent to the ionizing radiation.

At radio wavelengths, the advent of the VLA has made it possible to map the ionized gas distribution with a spatial resolution comparable to that of the infrared maps. A number of high spatial resolution radio maps of the thermal emission from the galactic center (Brown, Johnston, and Lo 1981; Brown and Johnston 1983; Ekers *et al.* 1983; Lo and Claussen 1983) indicate that at least some of the gas is contained in extended, larger scale features. These maps have led to different suggestions for the kinematics of the central region, among them being outflow from a central object (Brown 1982), spiral infall of molecular cloud matter toward the center (Ekers *et al.* 1983), and central illumination of matter orbiting about the center (Lo and Claussen 1983). Although these newer scenarios differ greatly among themselves, they all predict a systematic variation in velocity along the radio features, and recent measurements of the H76α velocity field (van Gorkom, Schwarz, and Bregman 1984) show that velocities do change regularly along several of the radio features. However, not all of the "clouds" have been subsumed into more extended features, and the overall kinematics of the ionized gas within a few

[1] Visiting Astronomer at the Infrared Telescope Facility, which is operated by the University of Hawaii under contract with the National Aeronautics and Space Administration.

parsecs of the galactic center remains an open question. In order to address this question, new observations were made of the [Ne II] emission from Sgr A West, with higher sensitivity than achieved previously. We report here on the results of these observations.

II. OBSERVATIONS

The observations were made in 1983 June and July with the NASA 3 m IRTF on Mauna Kea, using a modified version of the tandem Fabry-Perot grating spectrometer designed by Lacy (1979). Both the spectral and spatial resolutions are now adjustable while the dewar is cold. As a result, observations were possible with a spectral resolution ranging from 30 (FWHM) to 80 km s^{-1}, and with a beam size in the range 1".5 to 6". The noise-equivalent power (NEP) in a 6" beam and a 50 km s^{-1} (FWHM) bandpass was 1×10^{-14} W $Hz^{-1/2}$, an improvement of a factor of 2 over that achieved by Lacy *et al.* (1979).

The positions at which spectra were measured were chosen mostly to correspond to the distribution of radio emission. A map of the 5 GHz radio continuum emission (Lo and Claussen 1983) is shown in Figure 1, along with the beam positions to be discussed in this paper. A large number of additional spectra appear elsewhere (Serabyn 1984). In areas of weaker, more extended radio emission, spectra were measured with a 6" beam, while in regions of more intense emission 3" and 1".5 beams were used. Along the northern arm, the series of positions indicated in Figure 1 was observed with a 3" beam. The spacing between positions was 2".5, except for the four southernmost positions, where the spacing was 1".25. Beam positions were determined by peaking up on the [Ne II] emission from IRS 1 and offsetting from there. A chop of 2' E-W was used for all but the 1".5 beam observations, which required a smaller chop of 30" E-W. The measured flux was calibrated by comparison to the flux from α Sco, taken to be 1800 Jy at 12.8 μm. Line fluxes are accurate to $\pm 30\%$.

Frequencies were measured with respect to absorption lines of NH_3 in a sample cell. The resultant velocity scale is accurate to about ± 4 km s^{-1}. The largest source of error in the central velocity of emission seen at a position is often the pointing uncertainty. Although the pointing and tracking kept the beam on a given position to ~ 1" during our integration times of 2.5–10 minutes, in some locations an error of 1" could introduce a velocity shift of up to 10 km s^{-1}. Most discrepancies with the velocities measured by Lacy *et al.* (1980) are probably due to pointing differences.

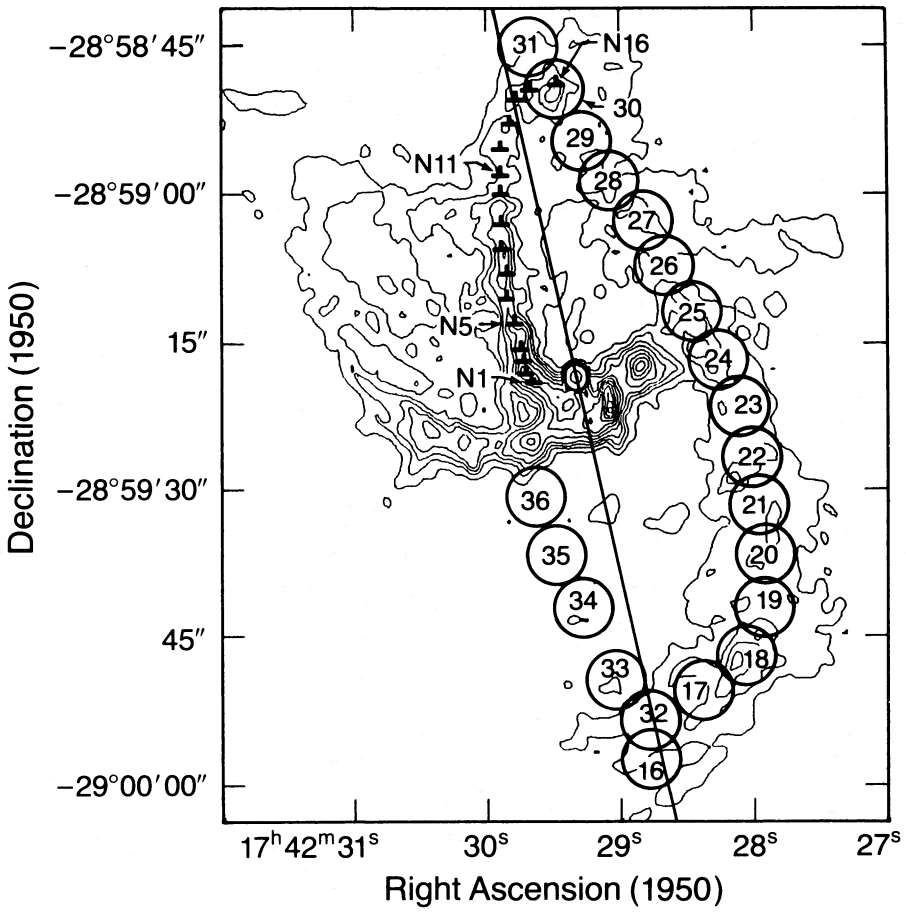

FIG. 1.—[Ne II] beam positions superposed on the 5 GHz map of Sgr A West (Lo and Claussen 1983). Circles correspond to our 6" beam positions, while the half-crosses refer to the 3" beams. Positions 16–31 comprise the "western arc." Reference line is perpendicular to the line connecting Sgr A* with the position on the western arc where the radial velocity crosses zero. For reference, IRS 1 is at position N2, IRS 8 is at N16, IRS 9 is just above position 36, and the "southern peak" is centered on position 18. IRS 16 is close to the radio point source at the center of the map.

III. RESULTS

a) The Northern Arm

The radio continuum feature which extends north-south for $\sim 25''$ along R.A. = $17^h42^m29^s.9$ has been referred to as the northern "arm" (Ekers *et al.* 1983). Previous observations of [Ne II] along this feature were interpreted as indicating the presence of a number of separate clouds, with velocities of 0, 50, and 90 km s^{-1} LSR, in addition to an extended component of emission. Recent H76α recombination line measurements in the same region show a regular velocity change along this feature from ~ 15 to ~ 100 km s^{-1} in a $10''$ distance (van Gorkom, Schwartz, and Bregman 1984). To discriminate between a continuous shift in the velocity of a single component and a continuous shift in the centroid of emission which is due to the strengthening and weakening of various emission components in the beam, new [Ne II] spectra were measured along the northern arm.

Spectra observed at positions N1 through N16 with a $3''$ beam and 30 km s^{-1} resolution are displayed in Figure 2, arranged in the order of the positions in the sky. One spectrum measured with a $1''.5$ beam halfway between positions N7 and N8 is also included. Also shown are computer-generated least-squares Lorentzian fits to the line shapes. For those spectra where more than one velocity component is evident or suggested, multicomponent Lorentzian fits were also tried, and in most cases, one or two Lorentzians were sufficient to fit the line shapes rather well. It is possible, however, that higher spectral resolution observations may resolve more components in a few of the positions.

Except for the southernmost spectrum, the spectra comprising the bottom half of Figure 2 (i.e., the southern $12''$ of the arm) show a single emission component, with central velocity which changes steadily with position. Comparison with the H76α map of van Gorkom, Schwarz, and Bregman (1984) shows good agreement. In this region there is no evidence that one velocity component weakens while another grows stronger as the position is varied. Thus, this section of the northern arm is better described as one coherent gas feature with a smooth gradient in radial velocity than as a series of independently moving clouds.

It is useful to ask how far in declination the northern arm can be followed via its velocity. The southernmost position shown has most of its emission at a velocity consistent with the gradient seen just to the north. Thus, the gas flow extends to within a few arc seconds of the 2 μm source IRS 16 (Becklin and Neugebauer (1968) and the radio point source Sgr A* (Fig. 1; Balick and Brown 1974), both candidates for the location of the center of the Galaxy. Going northward, a single velocity component is seen for $\sim 12''$. Beyond this point several components are seen, making it more difficult to follow a coherent feature, if present. The velocities from the least-squares fits to the spectra are shown in Figure 3 in a velocity-declination plot. This plot shows that a straight line rotation curve with a slope of 10.7 km s^{-1} arcsec^{-1} fits the seven southernmost positions adequately, although some curvature of the rotation curve appears to be present. Alternatively, a quadratic curve gives a better fit to these velocities and also fits a number of velocity components seen farther north. It appears that the organized flow extends to $18''$ N of the position of IRS 1, and possibly beyond. In addition to this flow, two other localized velocity features are notable. A cloud of ionized gas at -10 km s^{-1} is seen near IRS 8 (as discussed by Lacy *et al.* 1980), and a cloud

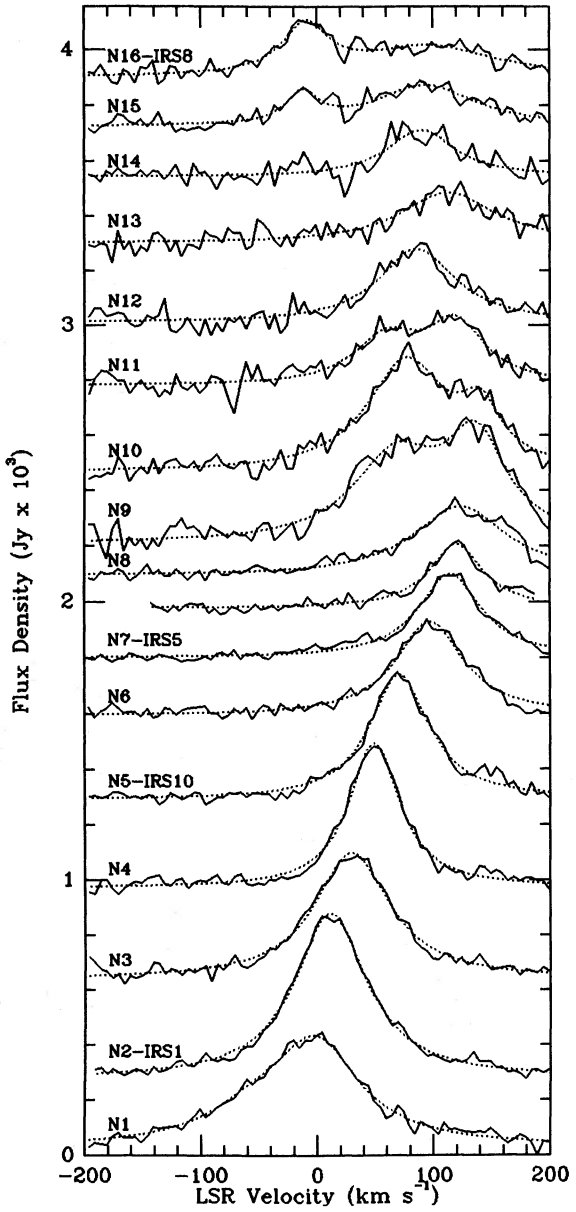

FIG. 2.—[Ne II] spectra measured along the northern arm, using 30 km s^{-1} resolution and a $3''$ beam. Also included between positions N7 and N8 is one spectrum measured between those positions with a $1''.5$ beam. The positions refer to Fig. 1. Also shown are Lorentzian best fits to the lines. Spectra N9–N16 are magnified 2.5 ×. Bin size is 5 km s^{-1}.

at about $+70$ km s^{-1} is seen halfway up the northern arm. This last cloud may not be part of the northern arm, since it seems to be associated with extended emission (Serabyn 1984).

A few spectra were also measured on the northern arm with a $1''.5$ beam , to determine if the measured line width near IRS 1 is caused by the large change in velocity across the beam. The FWHM measured at the position of IRS 1 with various beam sizes and spectral resolutions is plotted in Figure 4. As is evident in the figure, the measured FWHM of the line on IRS 1 varies linearly with the sum of the instrumental line width (FWHM in km s^{-1}) and the change in velocity along the northern "arm" subtended by the FWHM of the beam. Thus, much of the measured line width of the [Ne II] line on IRS 1

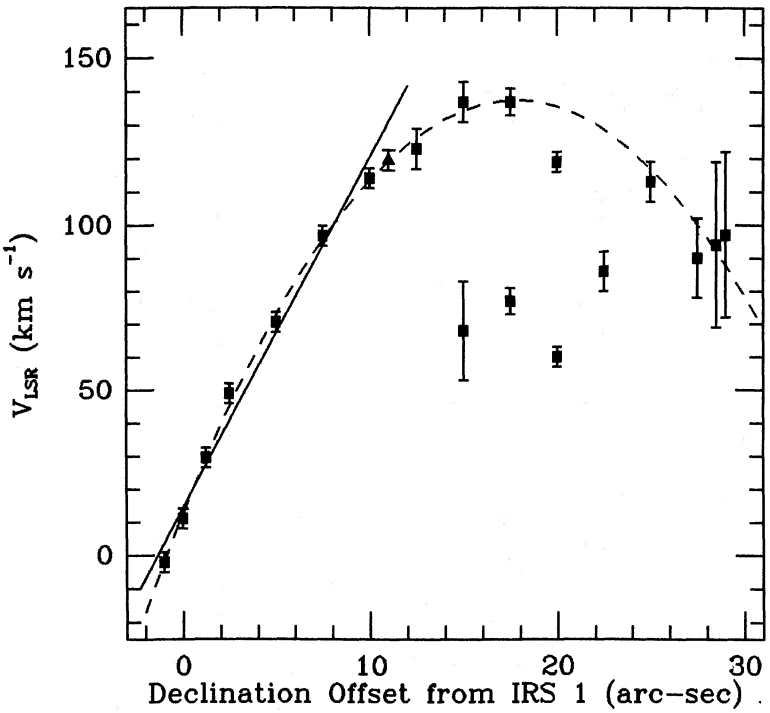

FIG. 3.—Best-fit velocities of the spectra along the northern arm vs. the offset (in declination) from IRS 1. The triangle refers to the 1".5 spectrum. The straight line is a least-squares fit to the first seven points, while the dashed curve is a least-squares quadratic fit to the first 10 squares. Large error bars appear where the signal-to-noise ratio is too low to rule out the presence of more than two components.

can be ascribed to both the beamwidth and the spectral resolution.

The linear relationship holds even with our smallest beam size and highest spectral resolution, implying that the line of sight FWHM is $\lesssim 46$ km s^{-1}. Extrapolating the linear relationship to infinite spatial and spectral resolution yields a FWHM of 26 km s^{-1}. Thus the line-of-sight velocity dispersion of IRS 1 is 36 ± 10 km s^{-1}, a downward revision of roughly a factor of 2 from previous measurements. The intrinsic line width at a point may, of course, be much smaller, if a gradient in velocity along the line of sight is also present. If this is the case, an intrinsic line width at a point consistent with thermal broadening cannot be ruled out, and locally the gas may behave as a normal H II region.

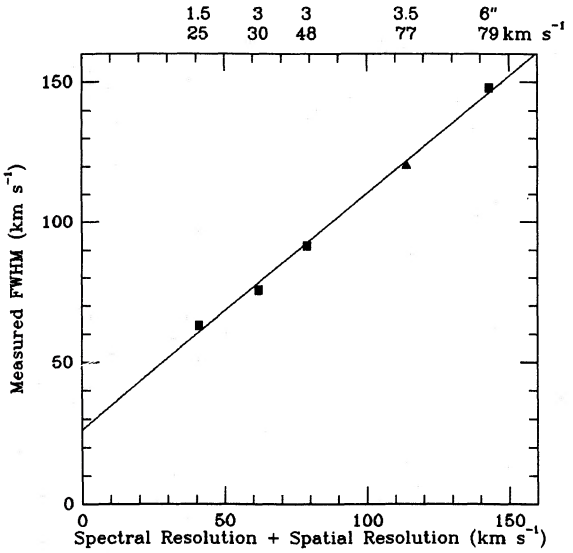

FIG. 4.—Measured FWHM of the [Ne II] line as a function of the sum of the instrumental FWHM plus the width of the beam in arc seconds × 10.7 km s^{-1} arcsec^{-1} (the gradient seen in Fig. 3). Squares are from this work; triangle is from Lacy *et al.* (1980). Top row of numbers gives the beam size; the next row gives the spectral resolution.

b) The Southern Arm

A second radio feature, located roughly at R.A. = $17^h42^m28^s$, with δ running from $-28°50'15''$ to $-28°59'55''$ has been referred to as the southern "arm." It has been suggested that this feature turns in toward the center at its northern end, making it part of a spiral pattern of emission centered roughly near Sgr A* and IRS 16 (Ekers *et al.* 1983). Alternatively, the feature could end near $\delta = 28°59'15''$, or it could continue on toward the north without changing its direction much, possibly terminating near IRS 8 (Lo and Claussen 1983). The weak radio continuum emission from the northern end of this arm makes it difficult, on the basis of intensity mapping alone, to determine the correct description of the gas morphology. [Ne II] spectra were measured along this feature to address this question.

Figure 5 shows [Ne II] spectra taken along the arc of positions 16–31 (shown in Fig. 1), which follows the southern arm and continues north to IRS 8. The spectral resolution used was 48 km s^{-1}. This series of positions will be referred to below as the "western arc." The spectra are shown in sequence; the bottom spectrum is the southernmost, and successive spectra move north along the western arc. A variation of the peak emission velocity with position is clearly present, the general trend being an increase from approximately -100 km s^{-1} LSR in the southernmost spectrum to approximately $+100$ km s^{-1} LSR in the northernmost spectrum. Several positions

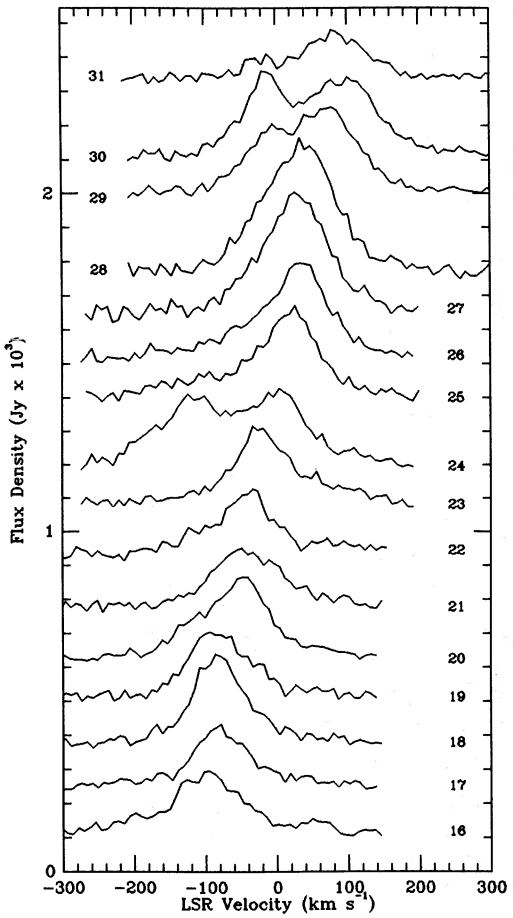

FIG. 5.—Spectra measured with a 6″ beam and 48 km s^{-1} resolution along the western arc (positions 16–31 in Fig. 1). Moving up in the figure corresponds to moving north along the arc. The bin size is 7.5 km s^{-1}.

measured on either side of the western arc agree with this trend (Serabyn 1984).

The fact that the velocity continues to change in a regular manner in continuing past the apparent northern end of the southern arm, with no decrease in [Ne II] intensity, implies that the arm does not turn in toward the center at this point, but is instead part of a longer feature which extends all the way north to IRS 8. The presence of a second, highly blueshifted component at position 24 and at no other nearby position along the western arc strengthens this argument. The second component, at -120 km s^{-1}, is very blueshifted compared to the velocities present at nearby positions along the western arc. This component of the emission is much more similar in velocity to the emission from the central "bar" region—the central region of strong emission running roughly E-W and already known to have highly Doppler-shifted emission (Lacy *et al.* 1980); in particular, -160 km s^{-1} emission is present in the nearest previously measured position (IRS 6). Highly blueshifted emission, with velocities exceeding -100 km s^{-1}, is also seen on the opposite side of the western arc (Serabyn 1984). Thus the -120 km s^{-1} component seen at position 24 can be associated with a highly blueshifted region which crosses the western arc at roughly a right angle and continues westward. We conclude, therefore, that the apparent spiral evident on the radio maps is due to a superposition along the line of sight of more than one structural feature. Kinematically, one feature follows the western arc shown in Figure 1 in a roughly north-south direction and goes through zero radial velocity near position 24. The second feature, with radial velocities exceeding -100 km s^{-1}, runs westward from the central region and crosses the western arc.

Figure 6 shows the best fit to the velocities of the main components in these spectra versus projected distance along a reference line (shown in Fig. 1) through the radio point source, Sgr A*. The orientation of this line was chosen so that zero velocity is projected approximately onto Sgr A*, but the results do not depend heavily on its exact orientation. This line differs by $\sim 20°$ from the plane of the galactic equator. As is evident from the straight line fitted to the points, the velocities along the western arc are consistent with gas moving in a circular orbit (seen as an ellipse in projection on the sky) about a center near the radio point source. The plane of the orbit is apparently tipped out of the plane of the galactic equator both along and perpendicular to our line of sight by comparable amounts. The slope of the best-fit line is 2.6 km s^{-1} arcsec^{-1}.

The change in velocity from spectrum to spectrum is not completely uniform, however. In a few locations, the velocity is constant for at least 6″. In other areas, the velocity changes smoothly from one position to the next, while in still other locations, stepping one beamwidth results in a large (~ 30 km s^{-1}) jump in velocity. Thus, in places, this flow contains clumps, or clouds, with large differences in velocity. This clumpiness is consistent with the appearance of the southern arm on the 5 GHz map of Lo and Claussen (1983).

Returning to Figure 5 for a closer examination of the spectra, we note that in several positions a second velocity component at a noncircular velocity is seen. In the north, near IRS 8, a velocity component is seen which appears at -25 km s^{-1} in the northernmost spectrum, and which gradually becomes redder in moving to the south. At position 28 this component appears only as a wider blue side to the line and has a velocity near 0 km s^{-1}. Thus the two clouds seen at ± 10 km s^{-1} in this region by Lacy *et al.* (1980) appear to be part of one larger cloud of ionized gas, with a variation in velocity along its length. Weaker secondary components can also be

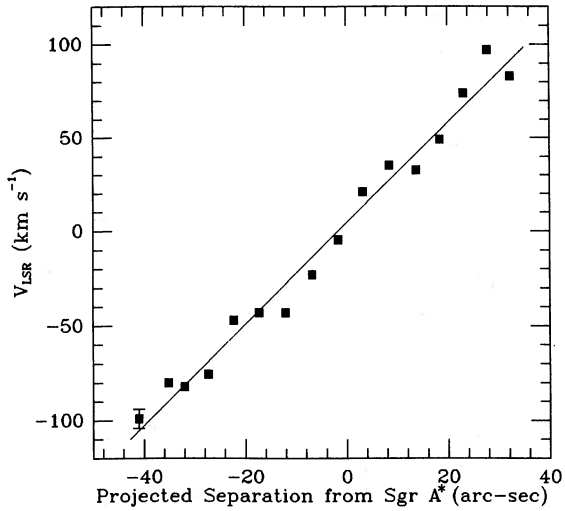

FIG. 6.—Best-fit velocities of the spectra along the western arc vs. the projection onto the straight line in Fig. 1 of the beam offset from Sgr A*. Also shown is a least-squares linear fit to the data. Slope is 2.6 km s^{-1} arcsec^{-1}. Typical error bars appear on the lowest point.

seen in spectra such as 20. Asymmetric line shapes in spectra 19 and 23, among others, suggest that these spectra also have secondary components at distinct velocities.

Although spectral resolution limits our information on the following point, there is some evidence that a number of spectra consist of distinct components, some of which fade in intensity and others of which grow in intensity as the position is varied. Thus the change in velocity of peak emission may not be due to the variation in velocity of a single, continuous gas stream, but may better be described as a change in velocity produced by stepping from a discrete cloud moving at one velocity to another cloud moving at a different velocity. For example, the main emission peak in spectrum 19 may turn into the weaker, bluer component in spectrum 20, while the extra emission on the red side of spectrum 19 may become the main peak in position 20.

To determine if the gas which appears to orbit about the center could actually be followed around the center, several spectra were observed along a strip from the southern peak to IRS 9 (positions 32–36 in Fig. 1). These spectra are shown in Figure 7. The neon line is 30% to 50% as intense in these spectra as it is along most of the southern arm, consistent with the 6″ resolution 5 GHz map of Brown and Johnston (1983). The velocity at the southernmost position in the strip (position 32) is -80 km s^{-1}. North of this position, the velocity decreases to about -35 km s^{-1}. Finally, in the northernmost spectrum, there is evidence of a 0 km s^{-1} component. (The 100–150 km s^{-1} emission in this spectrum is due to the edge of IRS 9.) Thus, the velocities in this region are reasonably consistent with rotation. Similarly blueshifted emission was also noted in this region by van Gorkom (private communication).

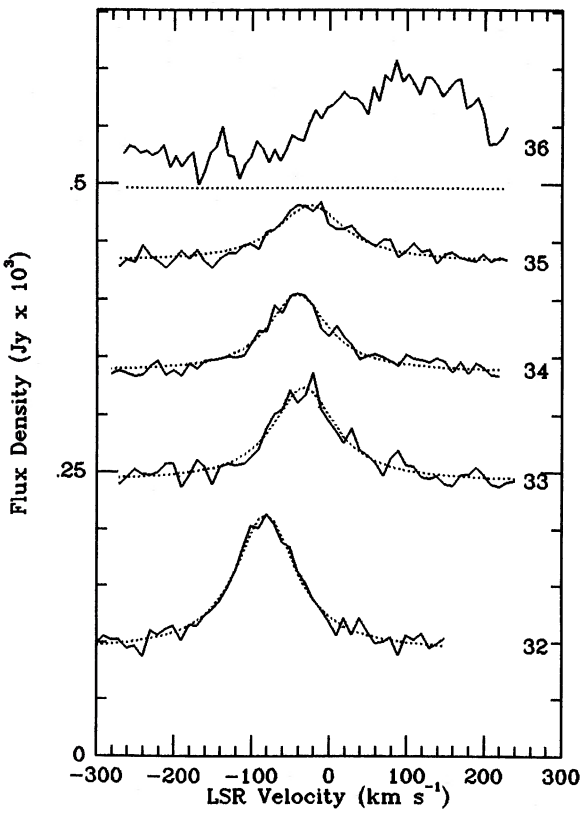

FIG. 7.—Spectra measured with a 6″ beam at positions 32–36 of Fig. 1. Spectral resolution is 48 km s^{-1}, and bin size is 7.5 km s^{-1}. No fit is included with spectrum 36 because of the presence of a number of unresolved emission components. Instead, the zero level for this spectrum is indicated. The 100–150 km s^{-1} emission in spectrum 36 is associated with IRS 9.

It has been suggested that the northern and southern arms are both part of one long inward spiraling orbit (Lo and Claussen 1983; Quinn and Sussman 1984). The suggested feature begins as the southern arm, continues north to IRS 8, and turns south again as the northern arm, spiraling ever closer to the center. The data reported here do not support this suggestion. Any model in which the gas along the western arc spirals inward would introduce an acceleration term into the rotation curve of the this gas. For example, the model of Quinn and Sussman predicts a velocity gradient which increases steadily from 2.6 km s^{-1} arcsec^{-1} on the southern peak to 10 km s^{-1} arcsec^{-1} at the northern turnover point. The data indicate that the southern arm and its northward extension to IRS 8 follow a linear rotation curve, with a rather constant velocity gradient of 2.6 km s^{-1} arcsec^{-1}. The velocity gradient along the northern arm is $\sim$4 times steeper, and it does have a nonlinear component. We conclude that the northern arm is not connected to the western arc or the southern arm, but is instead a separate flow of gas.

c) *The Bar and the Eastern Arm*

The bar region (the central emission region of Figure 1 running approximately E-W) was thoroughly mapped with a 3″.5 beam by Lacy *et al.* (1980). Therefore only a few preliminary spectra were measured here. These are presented elsewhere (Serabyn 1984), but the conclusions are summarized here. The broadest [Ne II] lines in the central region were resolved into multiple components with line widths $\lesssim$100 km s^{-1}, and as low as 35 km s^{-1} in some spectra. Up to four velocity features are present in some 3″ beam spectra. Spatial variations in the peak velocities of these components are seen. Furthermore, several 1″.5 beam spectra have succeeded in isolating a gas streamer with an extremely rapid variation in velocity (25 km s^{-1} arcsec^{-1}) and in tracing it from 0 to -170 km s^{-1} in the space of 7″. Thus, the central region of the bar contains several overlapping gas features, as indicated by the results of Lacey *et al.* (1980), but some of the velocity features have "streamer-like" variations in velocity.

The region to the east of the northern arm was mapped extensively with a 6″ beam (Serabyn 1984). Several redshifted emission components with spatial variations in velocity are present. Along the eastern arm (the narrow ridge on the 5 GHz map which runs eastward from the center and which gradually bends north), a number of emission components apparently overlap, making it difficult to trace individual features at the resolution used (48 km s^{-1}). The general trend along the eastern arm is one of increasing redshift as the center is approached. Correspondingly blueshifted gas is seen on the western half of the bar, extending beyond the western limit of the radio contours on Figure 1. Here also the trend is for an increase in velocity toward the center, but not all of the gas follows this trend.

The primary conclusion from this velocity mapping is that most of the ionized gas in Sgr A West is contained in extended, coherent gas flows, and not in independently moving clouds. However, it can still be argued that one or two of the velocity features on the bar may be in the form of a localized cloud. This applies primarily to the -260 km s^{-1} cloud, which appears localized in space and in velocity. This may, of course,

be due to insufficient spatial and/or spectral resolution, but it is not obvious that this cloud is part of a larger gas stream. Since the observations of the bar and the eastern region have not clarified the nature of the motions of these features, we shall discuss mainly the northern arm and the western arc in what follows.

IV. DISCUSSION

The velocities along the gas features discussed above provide information on the mass distribution in the central few parsecs of our Galaxy. The mass within the orbits of both the northern arm and the western arc are estimated below, and are used to address the question of whether or not a massive object, such as a black hole, is present at the center of our Galaxy. The presence of such a central black hole was suggested originally by Lynden-Bell (1969). Next, a simple model for the location of these ionized gas features is developed. Finally, the case for a single ionization source for the region will be examined.

a) Mass Estimate from the Western Arc

The velocities measured along the western arc were seen to be consistent with gas moving in a fixed radius circular orbit about the center. Since this rotating gas feature extends from the southern peak to IRS 8, a circular orbit (seen as an ellipse in projection on the sky) implies a radius of ~ 1.7 pc for the orbit, assuming a distance to the galactic center of 10 kpc. The shape of the southern arm then implies that the inclination between a normal to this circular orbit and the line of sight is $\sim 60°$–$70°$. With these parameters, we infer an orbital velocity of 110 km s^{-1}, assuming the line widths of 30–40 km s^{-1} are due to turbulence. This then implies a mass of $4.7 \pm 1.0 \times 10^6$ $M_\odot$ within a galactocentric radius of 1.7 pc.

This mass estimate agrees well with the mass estimated from the O I rotating about the center at radii $\gtrsim 1.5$ pc (Genzel *et al.* 1984, 1985) but is significantly below most of the mass estimates based on the statistical models of Lacy *et al.* (1980). This discrepancy can be ascribed primarily to the incomplete sampling of the velocity field at larger radii by Lacy *et al.* Their statistical mass estimate relies heavily on the high-velocity gas located close to the center. On the other hand, the mass estimate discussed here does not rely on a statistical argument, since the velocities along the western arc are well fitted by a simple circular orbit with known parameters.

How does the ionized gas along the western arc fit into what is already known about the distribution of gas and dust in the central few parsecs of the galaxy? Far-infrared observations have shown that warm dust is located in a ring which surrounds the center at radii $\gtrsim 1.5$ pc, and that the central few parsecs are relatively transparent to ionizing radiation (Becklin, Gatley, and Werner 1982). Lo and Claussen (1983) suggest that the northern and southern arms could be the ionized inner edge of molecular material near the center. Furthermore, the velocities of neutral oxygen in the dust ring indicate that the dust ring is rotating about the center (Genzel *et al.* 1984, 1985). Therefore, since the end points of the rotation curve of the western arc occur near positions located $\sim 34''$ north and south of the center, just inside of where the emission from the warm dust peaks, and since the circular orbital velocity of the ionized neon agrees well with the orbital velocity of the O I in the dust ring, the ionized gas seen along the western arc is most likely located on the inside edge of the ring of dust and neutral gas surrounding the central few parsecs.

This location implies that the source or sources of the ionization are centrally located, a result consistent with the conclusion of Becklin, Gatley, and Werner (1982) that the luminosity which heats the dust ring is primarily centrally concentrated. In this scenario, the ionizing photons generated in the central region are absorbed upon reaching the inner edge of the surrounding, circulating ring of gas. This location for the western arc is consistent with the observation that this gas flow seems to orbit at a fixed radius and justifies the use of the line center velocities in our mass estimate.

By combining the mass within the western arc's orbit with the bolometric luminosity of the central few parsecs, as measured in the far-infrared (1–3×10^7 $L_\odot$; Becklin, Gatley, and Werner 1982), the average $M/L_{\rm bol}$ ratio of the region within 1.7 pc of the center is found to lie in the range $0.15 < M/L_{\rm bol} < 0.5$. This assumes, as Becklin, Gatley, and Werner did, that the source or sources of luminosity lie within the central cavity in the dust ring. If the radial distributions of the source(s) of luminosity and the mass are different, the M/L ratio would, of course, be a function of radius. In contrast, the $M/L_{\rm bol}$ ratio of the bulge of our Galaxy has recently been estimated to be ~ 2 (Matsumoto *et al.* 1982). The lower $M/L_{\rm bol}$ ratio seen at the center probably reflects excess luminosity produced either by recent star formation, or by a more exotic central source.

b) The Northern Arm

The regular variation in velocity along the northern arm supports the view that this feature is a stream of gas following an orbit about the center. If its orbital radius is different from that of the western arc, the mass within a different distance from the center can be estimated. A comparison of the steepness and spatial extent of the two rotation curves indicates that the northern arm is, in fact, much closer to the center than the inner edge of the dust ring (very crudely, a factor of 3 or 4). However, since the velocity curve of the northern arm seems to rule out a simple circular orbit, the calculation of the mass within its orbit is not as straightforward. Therefore, to estimate the mass within its orbit, we attempted to fit three-dimensional orbits to both the radial velocity and position of the northern arm. A second question the model orbits can address is the orientation of the plane of the orbit of the northern arm. Finally, model calculations may help locate the center of our Galaxy.

Two simple models of the northern arm were explored numerically: Keplerian orbits about a central point mass, and orbits in an r^{-2} stellar density distribution. In the point-mass models, the distributed stellar mass is neglected. This assumption is not unreasonable if the point mass comprises upward of $\sim 3 \times 10^6$ $M_\odot$, since the estimated proximity of the northern arm to the center implies that the stellar mass remaining within the orbit would be a small fraction of the total central mass. Pressure in the gas stream is also neglected, and all of the gas particles are assumed to follow the same path.

An orbit more complex than a simple free-fall orbit is possible, if a medium capable of providing drag is present, as suggested by Quinn and Sussman (1984). Although no such medium has been detected to date, current observational constraints rule out only a medium with a temperature of $\lesssim 10{,}000$ K. However, the drag model assumes that only a single, initially localized gas cloud (initial cloud radius $\ll$ ring radius) is affected by the drag. If a drag medium were present throughout the region, the entire inner surface of the dust ring should be affected. Thus, rather than a single, discrete gas stream

approaching the center, a homogeneous inflow originating all along the inner surface of the dust ring would be present. Therefore, since the observed orbit of the western arc is quite consistent with a stable circular orbit, with no evidence of drag, the assumption of a simple drag-free orbit for the northern arm seems reasonable.

Other than the mass distribution, the parameters which completely determine the orbit are the location of the center, the energy and angular momentum of the orbiting particles, two angles describing the plane of the orbit, and one angle giving the orientation of the orbit in the plane. In order to fit an orbit to the data, a mass model, origin, energy, and angular momentum were selected, and the resulting orbit in a plane was calculated. The origin was defined by choosing its offset from IRS 1, taken to be coincident with the brightest [Ne II] position on the gas stream. An iterative least-squares fitting routine then rotated the calculted orbit in three-dimensional space by varying the three angles describing the orbit in order to determine their best values. For the case of Keplerian orbits, the program also varied the angular momentum (or the distance of closest approach).

Both the radial velocity and right ascension of the gas stream were treated as functions of the declination, and the fitting routine simultaneously fitted both sets of data. The relative weights assigned to the velocity and the positional data were chosen to ensure that both sets of data were being simultaneously fitted to reasonable accuracy. Only the data for the 10 southernmost positions (18″) that were observed along the northern arm were fitted. The data north of these positions were not included because of greater uncertainty in the velocity components present.

c) *Keplerian Orbits*

Since the rotation curve of the northern arm indicates a noncircular orbit, and since the northern arm has the qualitative appearance of a stream of gas approaching the central region of the Galaxy (Lo and Claussen 1983), the data were fitted with parabolic and hyperbolic orbits. Both types of orbit were found to fit the position and velocity of the northern arm well. The results for parabolic orbits are presented in detail.

Parabolic orbits were calculated for a number of origin locations near IRS 16, in order to determine the origin location which requires the least central mass to fit the data. This location is estimated to be $\sim 2\farcs7$ W and $\sim 1''$ N of IRS 1. With this origin, and a central mass of $4 \times 10^6\ M_\odot$, the position and velocity of the calculated orbit are nearly indistinguishable from the measured orbit of the section of the northern arm in consideration (Fig. 8*a* shows the velocity fit). As the central mass is decreased, the fit gets worse. Furthermore, moving the origin more than 1″ toward the west or south (Fig. 8*b*) noticeably increases the mass necessary to produce a good fit. On the other hand, moving the origin a few arcseconds eastward worsens the spatial fit, while moving the origin a few arc seconds northward worsens the velocity fit. Thus, to fit adequately the northern arm's orbit, a parabolic orbit requires a central mass of $\gtrsim 3.5 \times 10^6\ M_\odot$. Assuming that the brightest [Ne II] position along the northern arm and the Brγ source IRS 1 W (Storey and Allen 1984) are coincident in position, our best estimate for the location of the central mass is coincident, to an accuracy of $\sim 2''$, with the position of the 2 μm source IRS 16 NE. Thus, the fits favor the IRS 16 complex as the location of the central mass.

The inclination of the perpendicular to the orbital plane with respect to the line of sight also does not depend strongly on the location or size of the central mass, with most models having an inclination of 65°–80°. The inferred orbital plane is thus much closer to the line of sight than to the sky. This inclination is comparable to that of the inner edge of the dust ring. There remains, of course, a front-back ambiguity in the location of both gas features. However, in the plane of the sky, the northern and southern arms are on opposite sides of the center. Furthermore, since the ionizing radiation is expected to be isotropic, and since this radiation must be absorbed before reaching the neutral matter which should lie on both sides of the center, the total amount of ionized gas on both sides of the center should be comparable. Hence, it is reasonable to assume that the two arms are on opposite side of the center, with the conclusion then being that the two arms are probably in nearly the same plane.

Finally, most models estimated the distance of closest approach of the orbit, $r_{\rm min}$, to be ~ 0.5 pc. This result arises primarily from the near linearity of the northern arm's rotation curve in the vicinity of IRS 1 (Fig. 3), since approximating the linear section of the rotation curve ($\sim 10''$ angular extent) by a circular orbit implies a radius for the orbit comparable to its linear extent. Since $r_{\rm min}$ was usually near IRS 1, this large $r_{\rm min}$ implies that IRS 1 may be spatially farther from IRS 16 than its projection on the plane of the sky suggests.

As long as the central mass is confined within $r_{\rm min}$ of the center, the calculated orbits should be unaffected. Thus, the parabolic orbits actually indicate that $\gtrsim 3.5 \times 10^6\ M_\odot$ lies within 0.5 pc of the center. Hyperbolic orbits were also investigated in order to determine if an initial infall velocity could be responsible for the higher velocities seen on the arm. Orbits with initial velocities of 50 and 100 km s^{-1} provided good fits, and none of the conclusions differed from the case of a parabolic orbit. A similar central mass was still required to fit adequately the data. Apparently, although an initial infall velocity increases the velocity of the gas stream, the higher eccentricity opens up the orbit, so that the component of the velocity along the line of sight need not increase. Since these types of orbits proved adequate, elliptical orbits were not pursued. The higher velocities seen along the northern arm probably would have required a similar mass in this case also.

d) *Orbits in a Stellar Cluster*

A computer program was written to calculate orbits in the gravitational field produced by a stellar density distribution, $\rho(r)$, of the form $r^{-\alpha}$, for $0 < \alpha < 2$ (the details appear in Serabyn 1984). The origin was assumed to be at the best origin location determined above for Keplerian orbits. Orbits were first calculated for $\alpha = -1.99$, since this density distribution closely approximates the density distribution of an isothermal stellar cluster outside of the core radius (r^{-2}). No core was included because none is seen in the galactic center to a scale of $\lesssim 1''$ (Allen, Hyland, and Jones 1983). All orbits in such a mass distribution are bound. Of the possible orbits, only those extending far enough from the origin to cover the 10 southernmost positions observed along the northern arm were considered.

For ease in comparison to the observed value, the mass within 1.7 pc of the center is the quantity of interest and will be referred to as the "cluster mass" or as $M(1.7)$. The procedure for fitting the data was as follows. For a given choice of $M(1.7)$, orbital energy E, and angular momentum L, the fitting routine rotated the calculated orbit in three-dimensional space to find

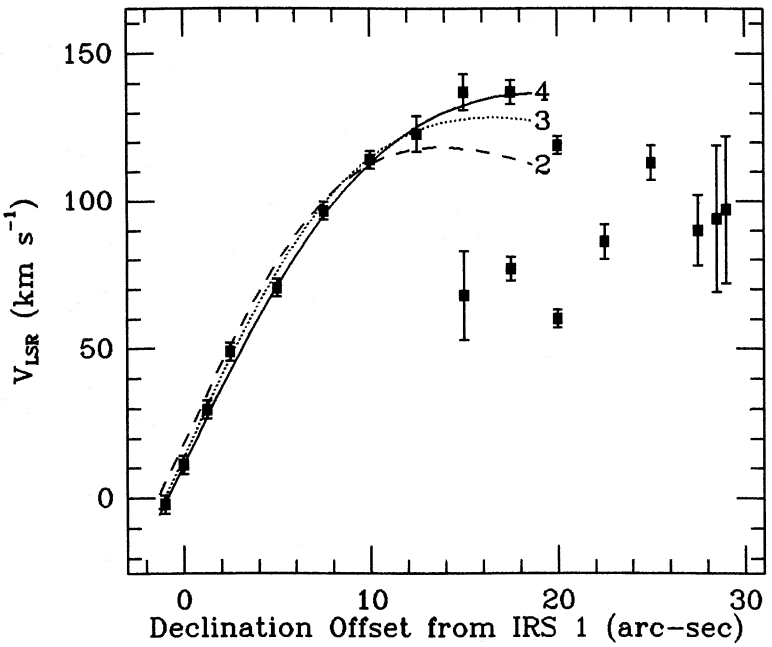

FIG. 8*a*

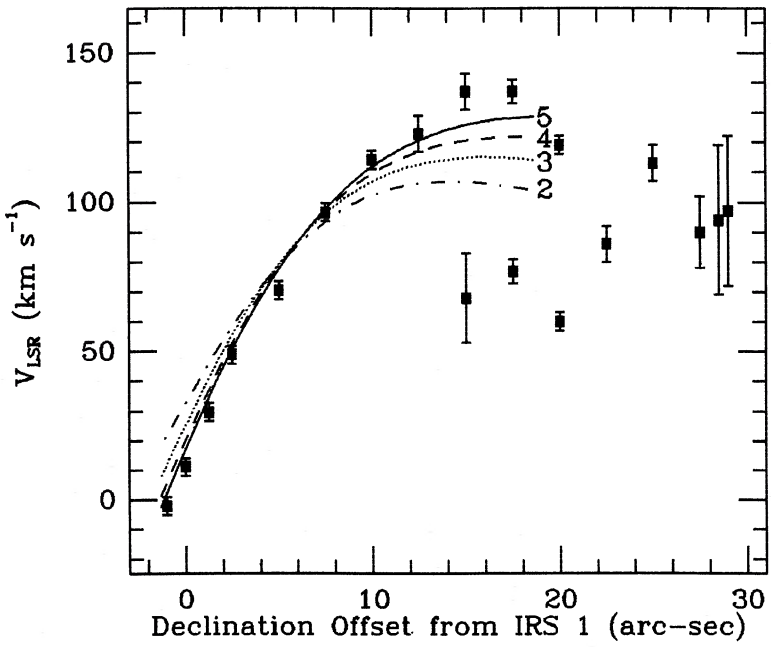

FIG. 8*b*

FIG. 8.—(*a*) Best-fit parabolic orbits about a point mass of 4, 3, and 2 × 10^6 $M_\odot$ located 2".7 W and 0".7 N of IRS 1 (~IRS 16 NE). (*b*) Best-fit parabolic orbits about a point mass located 5" W and 0".3 S of IRS 1 (~Sgr A*).

the best orientation. For a given $M(1.7)$, orbits with different combinations of E and L were fitted, in order to find the values of these parameters which produce the best fit to the observed orbit. The optimum values of E and L were determined for a number of cluster masses and were found to vary little with cluster mass. (The best value of r_{min} was again found to be ~0.5 pc, and an orbital r_{max}/r_{min} ratio of ~2.3 was found to fit the data well.) Thus, for purposes of comparing best-fit orbits with different cluster masses, E and L can be held constant near their optimum values.

The effect of varying the cluster mass with E and L optimized is shown in Figure 9. The primary conclusion apparent in the figure is that $M(1.7)$ must be $\gtrsim 11.5 \times 10^6$ $M_\odot$ to allow an orbit in an r^{-2} cluster to fit the northern arm's orbit. Such a high cluster mass substantially exceeds the observed mass within 1.7 pc of the center. This result can be understood as follows. For an r^{-2} density dependence, since the mass within a radius r is proportional to r, $M(1.7) \gtrsim 11.5 \times 10^6$ $M_\odot$ implies that $M(0.5)$, the mass within 0.5 pc of the center, is $\gtrsim 3.4 \times 10^6$ $M_\odot$. Since this mass agrees very well with the mass estimated

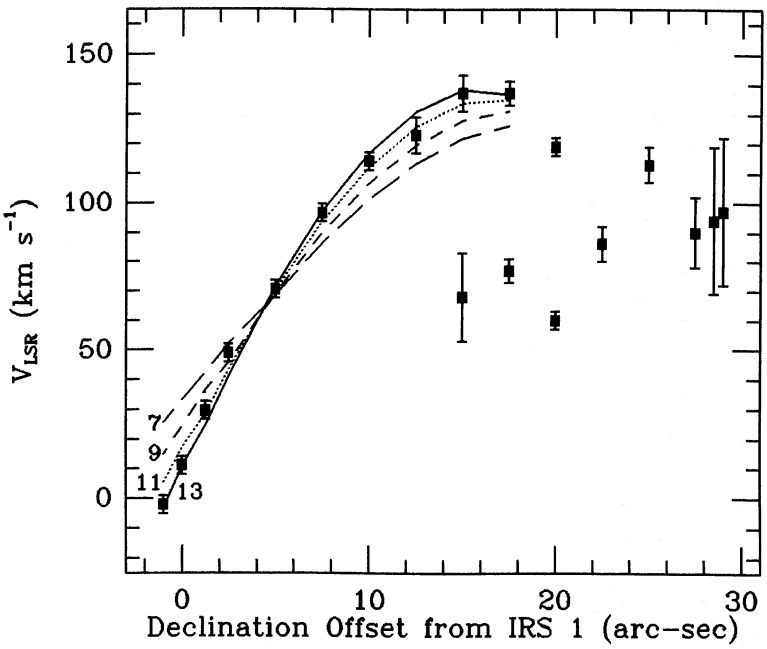

FIG. 9.—Best-fit orbits in a stellar cluster with an r^{-2} radial density variation. The assumed center is at the same position as in Fig. 8*a*. The orbits are labeled in terms of the cluster mass contained within 1.7 pc of the center.

to be within 0.5 pc of the center by fitting Keplerian orbits to the northern arm, it appears that the mass within the northern arm's orbit is relatively model independent. It is then the assumption that the mass is proportional to radius that produces an excessive mass within 1.7 pc of the center.

The stellar density distribution inferred from the 2.2 μm flux distribution from the central few pc, $\rho \propto r^{-1.7}$ (Becklin and Neugebauer 1968; Allen, Hyland, and Jones 1983), is even flatter than the assumed r^{-2} dependence, and would have an even larger ratio of $M(1.7)/M(0.5)$. To fit the orbit in this case would thus require an even larger cluster mass. Thus, no orbits were calculated for this case. For the same reason, a core in the stellar density distribution would also have required a larger cluster mass, and was therefore not pursued.

e) Mass Distribution

The mass estimates calculated above relied on the assumption that the distribution of the gravitating mass within 1.7 pc of the galactic center is spherically symmetric. While a nonspherical stellar distribution would affect our mass estimates, such a distribution seems improbable, given the smooth circular orbit of the western arc, unless this orbit lies in the symmetry plane of an ellipsoidal stellar distribution. Moreover, since the 2 μm stellar flux from the central 2 pc is not obviously nonspherical (Allen, Hyland, and Jones 1983), we shall assume that the stellar cluster at the galactic center is approximately spherically symmetric. Under this assumption, the western arc's orbit indicates that $4.7 \times 10^6\ M_\odot$ resides within ~ 1.7 pc of the galactic center, while the modeling of the northern arm's orbit indicates that $\gtrsim 3.5 \times 10^6\ M_\odot$ lies within 0.5 pc of the center. Therefore, most of the mass within the outer orbit also lies within the inner one.

The above conclusion is not based on a statistical argument or on the presence of a single high velocity, which can be produced by gas moving directly down the line of sight. It does rely on continuously tracing a single orbit along the northern arm from -2 to 137 km s^{-1}. This single velocity feature can easily be followed from -2 to 120 km s^{-1}, after which additional velocity components appear in the spectra. Larger beam (6″) observations (Serabyn 1984) are not completely conclusive but seem to indicate that the lower velocity features appearing in these spectra are associated with spatially extended emission, while the higher velocity gas is localized on the northern arm. Hence, it is reasonable to conclude that the 137 km s^{-1} component seen along the northern arm is the continuation of this gas stream. Certainly the radio continuum feature extends this far north. The conclusion further relies on the assumptions that the northern arm's orbit is not affected by drag and that all of the particles along the orbit follow the same path. As discussed earlier, the stable circular orbit of the western arc argues against the presence of a drag medium, and the northern arm's orbit can reasonably be expected to be drag-free.

The inferred mass distribution is too centrally concentrated to be due to a spherical isothermal stellar cluster, or to the stellar cluster inferred from 2 μm observations of the region ($\rho \propto r^{-1.7}$). The two orbits are consistent either with a stellar density distribution steeper than $\rho \propto r^{-2.7}$, or with a central point mass of $4 \pm 1 \times 10^6\ M_\odot$, or with a point mass of $\sim 3 \times 10^6\ M_\odot$ in combination with a cluster of $\sim r^{-2}$, containing a mass of $\sim 1.7 \times 10^6\ M_\odot$ inside of 1.7 pc. If the 2 μm flux from the region gives an accurate representation of the distribution of stellar mass present, a purely stellar cluster with $\rho \propto r^{-2.7}$ can be ruled out. This will be the case if the extinction to the galactic center at 2 μm does not distort the shape of the light distribution and if mass segregation (Illingworth and King 1977) of heavier stars to the center of the cluster does not decouple the stars containing most of the cluster's mass from those seen at 2 μm.

The uniformity in color of the near-infrared flux from approximately the central 100″ (Becklin and Neugebauer 1969) argues that the extinction to the central few pc is rather

uniform (Becklin *et al.* 1978), although a few small patches of excess extinction are seen (Allen, Hyland, and Jones 1983). Since the extinction at 2 μm does not appear to have a significant radial variation, at least over the central 2–3 pc, it does not appear capable of greatly altering the shape of the 2 μm light distribution.

For mass segregation to cause the total stellar density distribution to follow $r^{-2.7}$, while allowing the late-type giants seen at 2 μm to have a density distribution proportional to $r^{-1.7}$, most of the mass in the region would have to be in stars (or stellar remnants) heavier than those seen at 2 μm. However, a normal stellar population would be expected to have most of its mass in lower mass stars (Miller and Scalo 1979), i.e., stars not massive enough to have evolved to the giant phase yet. Thus, for the total stellar density distribution to be proportional to $r^{-2.7}$, a very unusual stellar population, heavily favoring massive, yet low-luminosity stars, would have to be present. Hence, mass segregation also does not appear capable of being the cause of a misleading 2 μm flux distribution.

Since the 2 μm flux indicates that the stellar density is approximately proportional to $r^{-1.7}$, the case of a stellar cluster with $\rho \propto r^{-2.7}$ is apparently ruled out. Thus, the central mass concentration in our Galaxy is most likely due to the presence of a massive central object. This massive object is presumably a black hole. The approximate agreement of the observed stellar density distribution with that expected near a massive black hole ($\rho \propto r^{-1.75}$; Bahcall and Wolf 1976) lends support to this conclusion.

The conclusion that most of the mass inside of $r = 1.7$ pc is in the form of a single massive object implies that there are $\lesssim 1.7 \times 10^6\ M_\odot$ of stars in the same volume. Although previous estimates of the stellar mass in the region were somewhat higher (Becklin and Neugebauer 1968; Sanders and Lowinger 1972), these estimates were based upon an uncertain mass-to-luminosity ratio (assumed to be ~ 3). As discussed earlier, the actual $M/L_{\rm bol}$ at the center of our Galaxy is $\lesssim 0.5$, much lower than previously assumed. Since a bulge-like M/L ratio is apparently inappropriate within a few parsecs of the galactic center, the lower stellar mass estimated above does not seem unreasonable.

f) The Bar

The velocities of the gas along the bar may provide another approach to the mass distribution. The observations of Lacy *et al.* (1980) revealed that the highest velocities (± 260 km s^{-1}) occur on the bar, within 5″ of the center. However, their observations did not include enough of the more distant gas to be certain that the velocity dispersion increases toward the center. The observations reported here do support such a conclusion, since the orbital velocity of 110 km s^{-1} measured at $r \approx 1.7$ pc is significantly less than the higher velocities seen closer to the center.

The nature of the motion of the ± 260 km s^{-1} clouds remains uncertain, but if they are in orbit about the center, their velocities are consistent with the presence of a massive black hole, while being statistically very improbable in an isothermal spherical stellar cluster. If the ± 260 km s^{-1} clouds are being expelled from a central object, its mass cannot be estimated by this procedure, but an unusual object is indicated. On the other hand, if the clouds are falling inward, either a black hole or a stellar cluster is possible. For infalling gas to be accelerated to 260 km s^{-1} in an r^{-2} stellar cluster, it must fall from an initial distance of $\gtrsim 3.5$ pc from the center and should be in the form of a long streamer. The relatively localized position and velocity of the -260 km s^{-1} cloud argues against infall producing this velocity feature, but not conclusively, since higher spatial resolution may succeed in resolving this gas clump.

Still closer to the center, broad helium and hydrogen emission have been detected toward IRS 16 (Hall, Kleinmann, and Scoville 1982; Geballe *et al.* 1984). The width of the line is ± 700 km s^{-1}, and the emission region is probably a few arc seconds in size. Geballe *et al.* (1984) note that this velocity dispersion is consistent with rotation at $r \approx 1''$–$2''$ about a black hole of mass $3 \times 10^6\ M_\odot$, but interpret the velocity spread instead in terms of an outflowing wind of gas being ejected from the center. It is not clear that the velocity spread is due to outflow, since the velocities are comparable to the escape speed from a black hole of that size at that radius, implying that the gas may be bound.

Taken together, the ionized gas on the inner edge of the dust ring orbiting at 110 km s^{-1}, the ± 260 km s^{-1} clouds $\sim 5''$ from the center, and the ± 700 km s^{-1} motions seen within 1″–2″ of the center indicate that the velocity dispersion increases toward the center by amounts appropriate to a central mass of $\sim 4 \times 10^6\ M_\odot$. If all these velocities are due to rotation, the case for a black hole is rather strong.

g) A Model for the Central 3 Parsecs

The earlier discussion indicated that the ionized gas along the western arc is most probably located on the inner edge of the ring of dust and neutral gas which orbits about the center at $r \gtrsim 1.7$ pc and that the source or sources of the ionization are located within the central cavity. If this location for the western arc is indeed correct, then the western arc outlines only half of the inner edge of the dust ring. If the dust rings's inner edge were perfectly circularly symmetric about a location within a few arc seconds of Sgr A*, the corresponding eastern half of the "ionized ring" should follow a curve from near IRS 8 in the north, to a point near IRS 4 on the eastern arm, and continue on to the southern peak. Such a feature is not apparent on the radio continuum maps. However, ionized neon emission has been detected in the southeastern quadrant, in the apparent gap in the ionized gas distribution between the eastern arm and the southern peak (Fig. 7). As discussed previously, the measured velocities are reasonably consistent with rotation about the center and, thus, do fit into the model.

In the northern half of the radio maps, the northern arm occupies a location a few arc seconds closer to the center (in projection on the sky) than the projection of a perfectly circular orbit would imply. Furthermore, the earlier discussion indicated that the northern arm is, in fact, at a smaller distance from the center than the dust ring and that the orbits of the two features are likely to lie in nearly the same plane, with the northern arm on the opposite side of the center from the southern arm. Therefore, the northern arm may be the gas feature in the northeastern quandrant which is closest to the center and is thus exposed to centrally produced ionizing photons. It is thus possible that the northern arm may shield the neutral gas located at larger galactocentric radii in the dust ring from centrally produced ionizing photons. Shielding of the more distant gas is also proposed by Gatley *et al.* (1984) to explain the distribution of shocked H_2.

A simple calculation suports the shielding hypothesis. The 5 GHz optical depth through the northern arm (~ 0.2; Brown, Johnston, and Lo 1981) can be used to calculate its emission

measure. Assuming that this gas streamer is illuminated by a central source which emits photons isotropically, and taking an average distance from the center of ~ 0.5 pc, the central flux of ionizing photons needed to produce this emission measure is $\sim 4 \times 10^{50}$ Lyman continuum photons s^{-1}, in good agreement with the total ionizing flux determined by the total 10 and 5 GHz thermal emission from Sgr A West (Pauls *et al.* 1976; Brown and Johnston 1983). Thus, if a central source (or a number of central sources localized within ~ 0.5 pc of the center) provides the ionization, the northern arm is capable of absorbing all of the ionizing photons emitted in its direction, allowing the gas behind it to remain neutral.

Returning now to the southeastern quadrant, the paucity of ionized gas there implies either that this quadrant contains very little gas, or that neutral gas is present but few ionizing photons are able to reach it. The first possibility implies that the dust ring orbiting about the center has a gap in it, as suggested by Lo and Claussen (1983). This alternative does not appear likely, in view of the large extent of the dust ring along the plane of the Galaxy, as determined by the distribution of neutral oxygen (Genzel *et al.* 1984, 1985). Differential rotation in a thick ring should leave some neutral matter in the southeastern quadrant. Furthermore, since O I emission has recently been seen in the southeastern quadrant (Genzel *et al.* 1985), it is likely that the dust ring is whole.

The alternative, namely, that few ionizing photons reach the neutral gas in this quadrant of the ring, implies that this section of the ring is somehow shielded from much of the ionizing flux. Now the only other gas features along the line of sight to the central regions occur on the bar. The rest of the central cavity should be relatively transparent to ionizing radiation. If one or some of the gas clouds along the bar are capable of keeping photons from reaching the southeastern part of the ring, then the source or sources of ionization must occupy a volume at least as small as the size of the bar. A distribution of OB stars occupying the entire central cavity and providing the ionization should have surface photoionized the gas in the southeastern quadrant to the same extent as the gas elsewhere on the inner surface of the dust ring. Thus, some rather centrally concentrated source of photoionization is indicated. The source could conceivably be a few clusters of OB stars along the bar, or perhaps a single object.

It is interesting to note that Sgr A* and IRS 16 are on the opposite side of the bar from the southeastern gas, allowing the possibility of shielding, if either were the source of much of the ionization. We can only speculate as to which gas feature on the bar could provide the necessary shielding between a localized ionization source and the southeastern quadrant and offer the following suggestion. On the 5 GHz map of Lo and Claussen (1983), the northern arm appears to bend around IRS 16 and Sgr A*. This may indicate that the northern arm extends far enough around the possible ionization source to keep photons from reaching the southeastern quadrant also.

A final point concerning the western arc is that its rotation curve contains regions of relatively constant velocity, as well as discontinuities in velocity of ~ 30 km s^{-1}. Thus, at least some of the dust ring consists of neighboring clouds with very different velocities. Since collisions between clouds with a relative velocity of ~ 30 km s^{-1} would produce molecular shocks (Kwan 1977), this mechanism may be important in producing the shocked molecular hydrogen emission which has been seen from the region of the dust ring (Gatley *et al.* 1984). This possibility is also discussed by Genzel *et al.* (1985). Differences which could distinguish between this suggestion and the central wind proposed by Gatley *et al.* (1984) arise in the extent into the dust ring of the shocked H_2, and the symmetry of the emission about the center. A central wind would be expected to shock mainly the inner surface of the ring, while collisions between clouds in the ring would presumably produce shocks much deeper into the ring. A central wind could also produce a very asymmetrical appearance to the H_2 emission if portions of the ring are shielded from the wind by intervening gas.

In summary, a model wherein the inside edge of the dust ring is centrally illuminated by ionizing photons is consistent with much of the data. The assumption that the ionizing source(s) is localized to $r \lesssim 0.5$ pc allows the gas at smaller radii (the northern arm and the bar) to shield the gas at larger radii (the dust ring) from some of the ionizing flux, possibly explaining the weakness of the emission from the eastern half of the ionized ring.

h) The Nature of the Northern Arm

As discussed previously, the northern arm seems to be following a simple eccentric Keplerian orbit. The orbits which fit best this gas stream indicate that its orbit need pass no closer to the center than 0.5 pc. This large distance of closest approach argues against a direct association of this gas with the central mass, and thus against ejection from a central source.

Whether the orbit of the northern arm originated on the inner surface of the dust ring or father out is presently uncertain. The inferred plane of the orbit is consistent with a dust ring origin, but the orbits which fit the data can extend further out. For material orbiting in the dust ring to be able to approach the center, friction or collisions must remove some of its angular momentum. The smooth circular orbit of the western arc implies that friction is probably not important. This is also indicated by the fact that the gas which does approach closer to the center (the northern arm) is in the form of a single gas stream, and not a homogeneous inflow originating along the entire circumference of the dust ring. Therefore, if the northern arm originated in the dust ring, a collision with a cloud moving at a very noncircular velocity must have taken place. Gas moving at a very noncircular velocity (roughly -10 km s^{-1}) is indeed seen near the northern extremity of the northern arm, near IRS 8. It is therefore conceivable that a collision between this gas cloud and the dust ring caused some of the ring material to lose angular momentum, resulting in the northern arm.

A ring origin for the northern arm, in combination with central illumination, suggests the possibility that neutral gas is associated with the northern arm itself. For example, the northern arm may merely be the ionized inner edge of a corresponding streamer of neutral gas. Support for such a suggestion comes from the observation that the neutral O I in the vicinity of Sgr A West shows velocity components similar to those present in the ionized neon (Genzel *et al.* 1985; Serabyn 1984). This seems to indicate that neutral gas is associated with the ionized gas located interior to the dust ring.

The fate of the northern arm is uncertain. A problem with the simple orbit hypothesis is that the gas should continue on past the center, yet only half of the orbit is seen. Several resolutions of this problem are possible. First, the gas stream may not have gotten any farher than IRS 1. Second, the orbit may continue on past the center, but the gas may not be ionized due to intervening matter between the radiation

source(s) and the gas. Third, the infalling gas may run into another gas cloud (on the bar?). This is suggested by the sudden change in direction that the northern arm seems to undergo at IRS 1 on the 5 GHz map of Lo and Claussen (1983). If this is the case, successive cloud-cloud collisions may be an important mechanism through which orbiting gas can lose angular momentum and fall closer to the center.

The proposed model, consisting of a centrally located ionizing source (confined to $r \lesssim 0.5$ pc) which illuminates the inside edge of the surrounding dust ring and the northern arm, accounts for a substantial fraction of the ionized gas seen in the central few parsecs of the galaxy. This gas apparently all lies in the plane of the dust ring. Excluding this gas (outlined with the beam positions in Fig. 1), much of the remainder lies roughly along the rotation axis of the dust ring, on the bar. The motion of the gas on the bar is of an uncertain nature and will not be addressed further, except to note that the location of the bar near the rotation axis of the dust ring is somewhat suggestive of ejection from a central source. This scenario has difficulties, however, in that the best candidates for the ejection source, IRS 16 and Sgr A*, are off to the side of the bar. Further observations to investigate the gas motions on the bar are planned.

i) The Source of the Ionization

Several recent results are supportive of the possibility of a single source providing a substantial fraction of the luminosity in the central few parsecs. Geballe *et al.* (1984) note that a source capable of ionizing the He^+ zone near IRS 16 would produce a Lyman continuum flux of 10^{49}–10^{50} s^{-1}. Henry, Depoy, and Becklin (1984) estimate the bolometric luminosity of IRS 16 center as 0.8×10^7 $L_\odot$. Since these values are not very far from the respective fluxes present, it is worth reexamining the question of whether a single source might be capable of exciting all of the ionized gas in the central few pc.

The chief arguments against a single source of ionizing photons can be found in Lacy *et al.* (1980). Owing to the low abundance of S^{+++} and Ar^{++} in Sgr A West, Lacy *et al.* concluded that a single source with a stellar spectrum could power all of the ionization in the central 3 pc only if its effective temperature satisfied $T_{\rm eff} \lesssim 31{,}000$ K. The problem with such a low $T_{\rm eff}$ is the low ratio of Lyman continuum to 2 μm flux that it implies. To produce all of the Lyman continuum flux needed to ionize the gas in Sgr A West without exceeding the observed 2 μm flux from any single source in the galactic center (excluding IRS 7) requires a higher $T_{\rm eff}$. Briefly, by considering one of the ionized gas clouds nearest the center, Lacy *et al.* calculated an upper bound on $\Phi_{\rm Hec}/\Phi_{\rm Lyc}$, the ratio of the number of flux of He ionizing photons to the number flux of H ionizing photons. Assuming $\Phi_{\rm Lyc} \approx 8 \times 10^{50}$ s^{-1}, they required that $\Phi_{\rm Hec}/\Phi_{\rm Lyc} \lesssim 7.5 \times 10^{-3}$. Using the model stellar atmospheres of Kurucz (1979), they concluded that this limit implies $T_{\rm eff} \lesssim 31{,}000$ K.

More recent estimates of $\Phi_{\rm Lyc}$ have indicated that $\Phi_{\rm Lyc}$ is lower than originally assumed, being $\lesssim 3$–4×10^{50} s^{-1} (Lacy, Townes, and Hollenbach 1982). Thus, $\Phi_{\rm Hec}/\Phi_{\rm Lyc}$ is actually $\lesssim 0.02$. Moreover, an error in the calculations of Lacy *et al.* (1980) led them to set their upper limit on $T_{\rm eff}$ too low. The tables of Kurucz (1979) indicate that a stellar spectrum with $T_{\rm eff} = 35{,}000$ K, $\log g = 5$ has $\Phi_{\rm Hec}/\Phi_{\rm Lyc} \approx 0.01$, approximately equal to the limit estimated by Lacy *et al.* Thus, to power all of the ionization in the central 3 pc, a single source needs satisfy only $T_{\rm eff} \lesssim 35{,}000$ K, higher than previously calculated.

A number of effects may alter the source spectrum, and so raise the limiting $T_{\rm eff}$ even more. First, an overabundance of metals at the galactic center would soften the source spectrum, as discussed by Balick and Sneden (1976). Assuming a single source with $L_{\rm bol} = 2 \times 10^7$ $L_\odot$ and $T_{\rm eff} = 35{,}000$ K, the magnitude of other effects on the spectrum can be estimated. If the emission were due to an optically thick sphere, its radius would be $\sim 8 \times 10^{12}$ cm. This is only a factor of 10 larger than the Schwarzschild radius of a black hole of mass 3×10^6 $M_\odot$. Thus, in the presence of a massive central object, the emission would be redshifted $\sim 6\%$, a small effect. On the other hand, the surface gravity would correspond to $\log g \approx 7$, larger than assumed in normal stellar atmosphere calculations. This larger $\log g$ could decrease $\Phi_{\rm Hec}/\Phi_{\rm Lyc}$ by nearly an order of magnitude, if an extrapolation of the calculations for $3.5 < \log g < 5$ (Kurucz 1979) to $\log g \approx 7$ is valid. This would allow $T_{\rm eff}$ to exceed 35,000 K by as much as 4000 K, without producing too many He ionizing photons and would further lower the ratio of 2 μm flux to Lyman continuum flux.

If accretion onto a black hole powers the emission, a sphere is probably not the most likely emission geometry. The actual sizes of these effects would be different with another geometry, but the effects would still be present. A face-on disk with a large diameter to thickness ratio is ruled out (Lacy, Townes, and Hollenbach 1982) because such a disk would have a large range of temperature across its surface. Requiring such a disk to produce all of the ionizing flux seen in the central few parsecs would result in the cooler parts of the disk producing more 2 μm emission than is seen from any single source in the galactic center, unless the disk is seen nearly edge-on, or unless the disk does not extend out to radii where the cooler material would lie (Lacy, Townes, and Hollenbach 1982). However, since the dust ring (and apparently also the northern arm) is within $\sim 20°$ of the galactic plane, there is reason to expect some alignment of the disk with the line of sight. This could reduce the expected 2 μm flux by a factor of ~ 3. Furthermore, since the inflow may not be steady state (Lacy, Townes, and Hollenbach 1982; Lo and Claussen 1983; Sanders and van Oosterom 1984), the disk need not be very extended. Cutting off the cooler parts of the disk would result in a spectrum similar to a stellar atmosphere, in that $T_{\rm eff}$ would be approximately constant. As discussed earlier, $T_{\rm eff}$ may be as high as $\sim 35{,}000$ K. Taking this as a representative value, a source with a stellar-type spectrum, $\log g \approx 5$, and a bolometric luminosity of 2×10^7 $L_\odot$ would produce 3–5 $\times 10^{50}$ Lyman continuum photons per second (Kurucz 1979; Panagia 1973), sufficient to ionize all of Sgr A West, while producing a 2.2 μm flux at the Earth of ~ 0.3 Jy (assuming the extinction at 2.2 μm is 2.7 mag.) This is just the flux seen from IRS 16.

Since IRS 16 has been resolved into three sources at 2.2 and 1 μm (Storey and Allen 1983; Henry, Depoy, and Becklin 1984), it is more appropriate to consider only the infrared flux from one component of IRS 16. Based on its 1 μm flux and an assumed $T_{\rm eff}$ of 31,000 K, Henry, Depoy, and Becklin (1984) estimate a bolometric luminosity for IRS 16 center of 0.8×10^7 $L_\odot$. Assuming instead a $T_{\rm eff}$ of $\sim 35{,}000$ K, its bolometric luminosity would be $\sim 10^7$ $L_\odot$. Furthermore, the higher $T_{\rm eff}$ would raise its Lyman continuum flux by more than a factor of 3, to 1.5–2.5 $\times 10^{50}$ s^{-1}, within a factor of 2 of that estimated for the region by Lacy, Townes, and Hollenbach (1982). Considering the factor of 2 uncertainties in the ionizing and bolometric luminosities present in the central 3 pc, as well as in the model atmosphere calculations, it is evident that a single

source of $T_{\rm eff} \approx 35{,}000$ K is not only consistent with the excitation of the gas in the central few parsecs, but also with the infrared flux observed from IRS 16 center, and the observed bolometric luminosity of the central few parsecs. Thus, in agreement with Henry, Depoy, and Becklin (1984), we conclude that a localized source, such as IRS 16 center, may provide a substantial fraction of the ionizing and bolometric luminosities present in the central few parsecs.

V. SUMMARY

1. The variation in velocity of the Ne II emission along several of the most prominent radio continuum features in Sgr A West indicates that at least two of the features (the northern and southern arms) are large-scale flows of ionized gas.

2. The flow along the southern arm continues all the way north to IRS 8, encircling the center of the galaxy in an arc of $\sim 180°$. The velocities along this "western arc" are consistent with pure circular rotation about the center. The mass interior to the orbital radius of ~ 1.7 pc is $4.7 \pm 1.0 \times 10^6\ M_\odot$.

3. Both the velocity and position along the northern arm are well fitted by a noncircular orbit with mass $\gtrsim 3.5 \times 10^6\ M_\odot$ within the orbital $r_{\rm min}$ of ~ 0.5 pc. We take this, combined with (2), as evidence for a central black hole of mass ~ 3–$4 \times 10^6\ M_\odot$. Our best estimate for the position of the central mass is coincident with IRS 16 NE to an accuracy of $\sim 2''$. The stellar mass inside of the dust ring is estimated to be $\sim 1.7 \times 10^6\ M_\odot$.

4. The western arc apparently lies on the inner edge of the rotating ring of dust and neutral gas which orbits the center at $r \gtrsim 1.7$ pc. The ionizing illumination must therefore originate inside the central cavity in the dust ring.

5. The northern arm appears to be the closest gas feature to the center in the northeastern quadrant of the dust ring. The northern arm may therefore shield the dust ring from the ionizing photons in this quadrant, producing an asymmetrical appearance to the ring. This would localize the source or sources of the ionization to within ~ 0.5 pc of the center. The southeastern quadrant of the ring may be similarly shielded from ionizing photons. If this is the case, the source or sources of the ionization must occupy a volume smaller than that occupied by the bar.

6. The simple orbits which fit the western arc and northern arm indicate that this arm is probably not spiraling inward. However, cloud-cloud collisions may provide a mechanism through which orbiting gas can lose angular momentum and fall closer to the center.

7. A single source with $T_{\rm eff} \approx 35{,}000$ K and $L_{\rm bol} \approx 10^7\ L_\odot$ is consistent with the total ionizing luminosity in the central 3 pc, the ionization state of the gas, the bolometric luminosity of the central few parsecs, and the near-infrared flux from IRS 16 center. Thus a localized ($r \lesssim 0.03$ pc) ionizing source may provide a substantial fraction of the ionizing and bolometric luminosities present in the central few parsecs of the Galaxy.

We would like to thank C. H. Townes for suggesting these observations, as well as for many helpful discussions and suggestions on this manuscript. We also thank R. Genzel, F. H. Shu, and I. R. King for many useful discussions, and K. Y. Lo and J. H. van Gorkom for providing data prior to publication. Finally, we thank the staff of the IRTF for their assistance. This work was supported by NASA grants 05-003-272 and 05-003-497 and NSF grant AST 82-12055.

REFERENCES

Allen, D. A., Hyland, A. R., and Jones, T. J. 1983, *M.N.R.A.S.*, **204**, 1145.
Bahcall, J. N., and Wolf, R. A. 1976, *Ap. J.*, **209**, 214.
Balick, B., and Brown, R. L. 1974, *Ap. J.*, **194**, 265.
Balick, B., and Sneden, C. 1976, *Ap. J.*, **208**, 336.
Becklin, E. E., Gatley, I., and Werner, M. W. 1982, *Ap. J.*, **258**, 135.
Becklin, E. E., Matthews, K., Neugebauer, G., and Willner, S. P. 1978, *Ap. J.*, **220**, 831.
Becklin, E. E., and Neugebauer, G. 1968, *Ap. J.*, **151**, 145.
———. 1969, *Ap. J. (Letters)*, **157**, L31.
———. 1975, *Ap. J. (Letters)*, **220**, L71.
Brown, R. L. 1982, *Ap. J.*, **262**, 110.
Brown, R. L., and Johnston, K. J. 1983, *Ap. J. (Letters)*, **268**, L85.
Brown, R. L., Johnston, K. J., and Lo, K. Y. 1981, *Ap. J.*, **250**, 155.
Brown, R. L., and Liszt, H. S. 1984, *Ann. Rev. Astr. Ap.*, **22**, 223.
Ekers, R. D., van Gorkom, J. H., Schwarz, U. J., and Goss, W. M. 1983, *Astr. Ap.*, **122**, 143.
Gatley, I., Jones, T. J., Hyland, A. R., Beattie, D. H., and Lee, T. J. 1984, *M.N.R.A.S.*, **210**, 565.
Geballe, T. R., Krisciunas, K., Lee, T. J., Gatley, I., Wade, R., Ducan, W. D., Garden, R., and Becklin, E. E. 1984, preprint.
Genzel, R., Watson, D. M., Crawford, M. K., and Townes, C. H. 1985, preprint.
Genzel, R., Watson, D. M., Townes, C. H., Dinerstein, H. L., Hollenbach, D., Lester, D. F., and Werner, M. 1984, *Ap. J.*, **276**, 551.
Hall, D. N. B., Kleinmann, S. G., and Scoville, N. Z. 1982, *Ap. J. (Letters)*, **262**, L53.
Henry, J. P., Depoy, D. L., and Becklin, E. E. 1984, *Ap. J. (Letters)*, **285**, L27.
Illingworth, G., and King, I. R. 1977, *Ap. J. (Letters)*, **218**, L109.
Kurucz, R. L. 1979, *Ap. J. Suppl.*, **40**, 1.
Kwan, J. 1977, *Ap. J.*, **216**, 713.
Lacy, J. H. 1979, Ph.D. thesis, University of California, Berkeley.
Lacy, J. H., Baas, F., Townes, C. H., and Geballe, T. R. 1979, *Ap. J. (Letters)*, **227**, L17.
Lacy, J. H., Townes, C. H., Geballe, T. R., and Hollenbach, D. J. 1980, *Ap. J.*, **241**, 132.
Lacy, J. H., Townes, C. H., and Hollenbach, D. J. 1982, *Ap. J.*, **262**, 120.
Lo, K. Y., and Claussen, M. J. 1983, *Nature*, **306**, 647.
Lynden-Bell, D. 1969, *Nature*, **223**, 690.
Matsumoto, T., Hayakawa, S., Koizumi, H., Murakami, H., Uyama, K., Yamagami, T., and Thomas, J. A. 1982, in *The Galactic Center*, ed. G. R. Riegler and R. D. Blandford (New York: Am. Inst. Phys.), p. 194.
Miller, G. E., and Scalo, J. M. 1979, *Ap. J. Suppl.*, **41**, 513.
Oort, J. H. 1984, in *IAU Symposium 106, The Milky Way Galaxy*, ed. H. van Woerden, W. B. Burton, and R. J. Allen (Dordrecht: Reidel), in press.
Pauls, T., Downes, D., Mezger, P. E., and Churchwell, E. 1976, *Astr. Ap.*, **46**, 407.
Panagia, N. 1973, *A.J.*, **78**, 929.
Quinn, P. J., and Sussman, G. J. 1984, preprint.
Rieke, G. H., and Low, F. J. 1973, *Ap. J.*, **184**, 415.
Sanders, R. H., and Lowinger, T. 1972, *A.J.*, **77**, 292.
Sanders, R. H., and van Oosterom, W. 1984, *Astr. Ap.*, **131**, 267.
Serabyn, E. 1984, Ph.D. thesis, University of California, Berkeley.
Storey, J. W. V., and Allen, D. A. 1983, *M.N.R.A.S.*, **204**, 1153.
Townes, C. H., Lacy, J. H., Geballe, T. R., and Hollenbach, D. J. 1983, *Nature*, **301**, 661.
van Gorkom, J. H., Schwartz, U. J., and Bregman, J. D. 1984, in *IAU Symposium 106, The Milky Way Galaxy*, ed. H. van Woerden, W. B. Burton, and R. J. Allen (Dordrecht: Reidel), in press.

J. H. LACY: University of Texas, Department of Astronomy, Austin, TX 78712

E. SERABYN: University of California, Department of Physics, Berkeley, CA 94720